Review

Advances in Mechanical Engineering

Advances in Mechanical Engineering
2018, Vol. 10(10) 1–12

DOI: 10.1177/1687814018802904
journals.sagepub.com/home/ade
SAGE

Experimental measurements of the flow field around a film-cooled blade leading edge using particle image velocimetry

José Omar Dávalos Ramírez[1], Juan Carlos García Castrejón[2], Francisco Carrillo Pereyra[1], Carlos Ponce Corral[1], Carlos Felipe Ramírez Espinoza[1] and Arturo Paz Pérez[3]

Abstract

In this article, particle image velocimetry studies were conducted in a low-speed wind tunnel to investigate the effects of blowing ratio and blade span in terms of the characteristics of the flow field around a film-cooled blade leading edge. The measurements were performed at 20%, 40%, 60%, and 80% of blade span and blowing ratios of M = 0.5, M = 0.75, M = 1, M = 1.5, and M = 2. Velocity, turbulence intensity, and structure of vortices during the interaction between cooling flow and mainstream were analyzed in detail. The analysis shows a significant increase in mainstream velocity at low blowing ratios, $M < 1$. Peaks of turbulence were observed at low- and high-span locations. Aerodynamical losses are expected at higher blowing ratios due to the formation of secondary vortices near the outgoing jet. These vortices were a consequence of velocity gradients at this zone.

Keywords

Film cooling, particle image velocimetry, vortex structures, turbulence intensity, blowing ratio

Date received: 20 November 2017; accepted: 30 August 2018

Handling Editor: Takahiro Tsukahara

Introduction

One of the ways to improve the performance of gas turbines is to increase the temperature of mainstream flowing through turbine blades. This temperature can reach up to 1500°C and has a negative impact on the structural integrity of the first stage blades, especially at the leading edge which is considered the most critical zone due to its exposition to high thermal loads.[1] To maintain the blade temperature below the material melting point, a film cooling technique is employed. In this technique, air (used as cooling flow) is ejected through discrete holes on the blade surface creating a layer which avoids its contact with the hot mainstream.

The effectiveness of the film cooling technique is influenced by characteristics of mainstream and cooling flows, such as the blowing ratio, the velocity ratio, the density ratio, the temperature ratio, and the free stream turbulence, among others. In addition, geometrical factors also affect the film cooling effectiveness: the diameter of the cooling holes, the angle of injection, the

[1]IIT-DMCU, Universidad Autónoma de Ciudad Juárez, Ciudad Juárez, Mexico
[2]Universidad Autónoma del Estado de Morelos, Cuernavaca, Mexico
[3]IIT, Universidad Autónoma de Ciudad Juárez, Ciudad Juárez, Mexico

Corresponding author:
José Omar Dávalos Ramírez, IIT-DMCU, Universidad Autónoma de Ciudad Juárez, Av. Del Charro 450, Col. Partido Díaz, 32310 Ciudad Juárez, Chihuahua, Mexico.
Email: jose.davalos@uacj.mx

shape of the injection hole, the blade-wall curvature, and so on.

Among the above parameters, the blowing ratio, $M = v_c\rho_c/v_m\rho_m$, is extremely critical because it defines the amount of mass flow used to cool the blade. Low blowing ratios will not guarantee an adequate coverage of blade surface, whereas large blowing ratios could cause the jet lift off from blade surface.[2,3] Another fact that must be taken into consideration is the amount of air used in film cooling from the compressor results in a reduction in overall turbine efficiency. The interaction between coolant jet and mainstream is highly three-dimensional in the zone near to the leading edge forming different types of vortical structures.[4–7]

Several investigations have been carried out to study the flow field using intrusive techniques like hot wire probes.[8–11] However, due to the nature of this technique, it is complicated to obtain a spatial resolution of the flow field during the mixing of mainstream and cooling flow. Pietrzyk et al.[12,13] performed a study using laser Doppler velocimetry (LDV), to know the effects of both the unit density ratio and the high-density ratio on a flat plate. Their results showed high turbulence levels when separation of film cooling occurs. Flow field measurements were done by Thole et al.[14] by means of LDV to compare the influence of film cooling holes with and without expanded exits. They found that peak turbulence levels occur at different locations. In geometries with expanded exits, peaks appeared at the exit of the cooling hole, whereas in geometries without expanded exits, peaks were located downstream the hole exit.

In addition to hot wire probes and LDV, particle image velocimetry (PIV) is another technique widely used in the study of the film cooling flow field. It has advantages because it is possible to capture planes in both two and three dimensions. Using PIV, Eberly and Thole[15] found that counter-rotating vortex pairs (CRVPs) have effects on the velocity near to the wall of the hole edges. Also, they found the breakdown of Kelvin–Helmholtz in the jet-to-free stream shear layer. Wright et al.[16] investigated the effects of free stream turbulence intensity on the film jet cooling structure and surface effectiveness using PIV and pressure sensitive paint, respectively. Their results showed that the mixture of coolant jet and mainstream increases at elevated free stream turbulence levels which affect the blade cooling. Zheng and Hassan[17] investigated the flow field downstream of a nozzle shape cooling hole on a flat plate using PIV with blowing ratios from $M = 0.5$–2. They found that streamwise vorticity average drops 55% at blowing ratio of $M = 0.5$ in comparison with cylindrical cooling holes, whereas at blowing ratios up to 1, the average drops around 30%–40%. Vortical structures were visualized by Song et al.[18] by means of PIV, on a flat plate with the addition of a vortex generator located at one-dimensional (1D) downstream the film cooling hole varying injection angle and blowing ratios. They reported an increment of 248% in the area averaged film cooling effectiveness with an injection angle of 20° and blowing ratio of $M = 1.5$. Effects of Barchan dune–shaped ramps in film cooling were studied by Zhou and Hu[19] using PIV. They reported the formation of anti-CRVP and consequently a reduction in the detachment of coolant flow over blade surface.

Kukutla and Prasad[20] investigated secondary flow on stagnation row of a combined impingement and film-cooled high-pressure gas turbine nozzle guide vane using PIV technique, where the mass flow rates used were 0.0032, 0.0045, and 0.0054 kg/s. In addition, the results obtained were validated using computational fluid dynamics (CFD) techniques; in this study, results such as non-linear velocity variations associated with counter-rotating vortices within the film hole and influence of static pressure on cooling distribution were found. More coolant moves toward the downstream rows of the leading edge, where the external surface static pressure is relatively lower. In this investigation, it is also reported the decrement of the coolant velocity when there is a high mainstream Reynolds number.

Most of the investigations about film cooling are made on flat plates, and the obtained results give a good approximation of film cooling. However, due to the complexity of the phenomena at the leading edge, information about flow characteristics along blade span is sparse. This work employs PIV technique to measure flow field near the leading edge of a gas turbine blade model. Measurements were performed in a low-speed wind tunnel. Blowing ratio was varied from $M = 0.5$ to 2 at four span positions (20%, 40%, 60%, and 80%). The results achieved were analyzed in terms of velocity, turbulence intensity, and vorticity.

Experimental facilities

The experiments were conducted in a subsonic wind tunnel. By means of PIV, measurements of flow field were obtained around the leading edge of a gas turbine blade cylindrical model. The test rig used is presented in Figure 1. The test section is $0.5\,m \times 0.5\,m \times 0.25\,m$. Air from the exterior was supplied by an axial fan placed at the end of the wind tunnel; it passes through a flow straightener to correct circulation. Smoke particles were generated inside a seeding box (made of Plexiglas); the seeding particles are oil drops in the range of 1–5 μm, and then these particles were distributed at high pressure, by means of a compressor, to the plenum and the mainstream inlets, where the smoke particles mix with the air supplied by the axial fan. To monitor air velocities at the mainstream and plenum inlets, a system

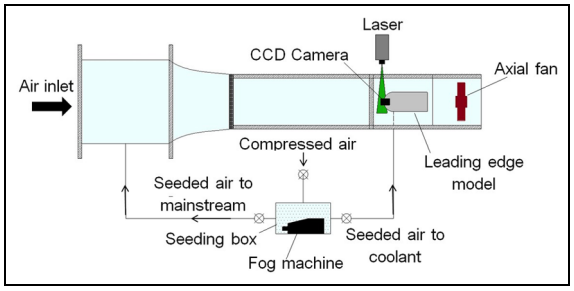

Figure 1. Experimental rig.

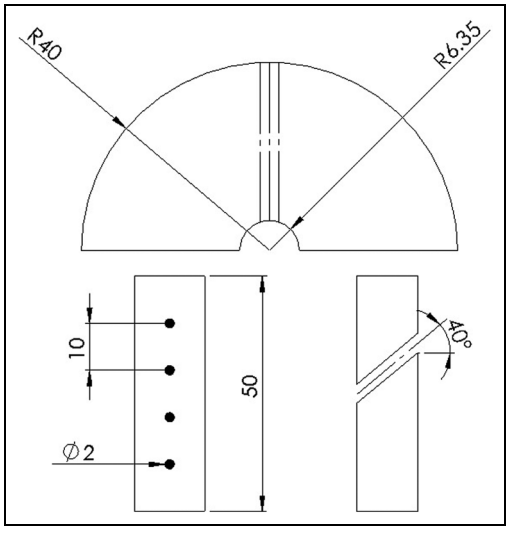

Figure 2. Leading edge model dimensions (mm).

of hot wire anemometer probes was placed at these locations. The signals were sent to an acquisition card for its processing and were shown on a PC during PIV measurements.

The air entered the tunnel with a velocity of 10 m/s. The free stream Reynolds number at leading edge was 80,296 (based on the half perimeter of the leading edge model). In this research, the density ratio between the coolant and the mainstream was considered to be 1.

A cylindrical leading edge model was built with a single row of four cylindrical cooling holes at leading edge. The span of the row of holes was 50 mm. The model has a semi-circular cylinder shape with 80 mm diameter and with a plenum of 12.7 mm diameter. The cylindrical holes have a diameter of 2 mm, a pitch of 10 mm, and an inclination of 40° in span-wise direction. The semi-circular chord has a length of 125 mm (Figure 2).

The PIV technique is a non-intrusive technique based on the displacement of tracer particles from one point to another in an interest zone which is illuminated by a laser sheet placed perpendicularly to a high-speed camera. The camera, synchronized to the laser pulses, records two images with a Δt between them. The images are divided into small subsections Δx called interrogation areas, and then velocity vectors are derived from $v = \Delta x/\Delta t$.

In this research, the tracer particles were illuminated by a double-pulsed Nd: laser with a double cavity. The dimensions of the interrogation and the target area were 64×64 pixels and $105\,\text{mm} \times 80\,\text{mm}$, respectively. The time between pulses was set to $3.3\,\mu\text{s}$, whereas the sampling frequency was set to 10 Hz. A CCD camera with a spatial resolution of $128.0\,\text{mm} \times 102.4\,\text{mm}$ was used to acquire the images. The distance between the camera and the laser sheet was about 1 m. The synchronization between laser and camera was made by means of a Dantec System Hub. The size of the particles seeded was 1–5 μm. A total of 500 image pairs were recorded for each measurement; this number of image pairs was selected based on the comparison of mean velocity between 500 and 600 image pairs, where the difference between them was less than 1%. The estimation of uncertainty at a 95% of confidence level based on mean velocity was estimated to be 0.1 m/s, whereas considering velocity vectors, the uncertainty was less than 0.2 m/s.[21] The image pairs were analyzed using the cross-correlation algorithm.

The measurements were carried out at $M = 0.5$, 0.75, 1, 1.5, and 2 with a cooling mass flow rate of 0.00310, 0.00465, 0.00620, 0.00930, and 0.0125 kg/s, respectively. Data were acquired in four horizontal planes, C1, C2, C3, and C4, located at 20%, 40%, 60%, and 80% of span blade, respectively. These locations were aligned with the center of each cooling hole. Two circumferential profiles were traced at 0.25D and 0.5D around leading edge. The portion of the measured chord was 97.06 mm. An additional profile was added to measure velocity from jet discharge to mainstream. The locations of planes and profiles are presented in Figure 3. An example of the PIV measurements is presented in Figure 4.

Results

A study about the interaction between mainstream and coolant flow in a row of cooling holes of a leading edge model at different span positions was made using PIV. Blowing ratio was varied at values of $M = 0.5$, $M = 0.75$, $M = 1$, $M = 1.5$, and $M = 2$. The behavior of velocity, turbulence intensity, and vorticity has been investigated. Due to symmetry conditions, only half of the model was presented.

Velocity variations from the jet exit to the mainstream are plotted in Figure 5. When $M = 0.5$, the amplitude of velocity peaks is minimal at C1 but becomes higher as the span increases. The length of the fluctuation at C4 is larger than at the other positions in all blowing ratios that were analyzed. The variation at

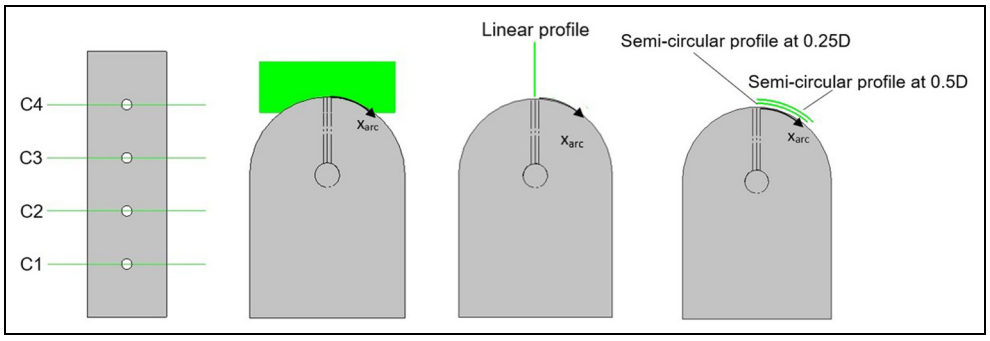

Figure 3. Locations of planes and profiles.

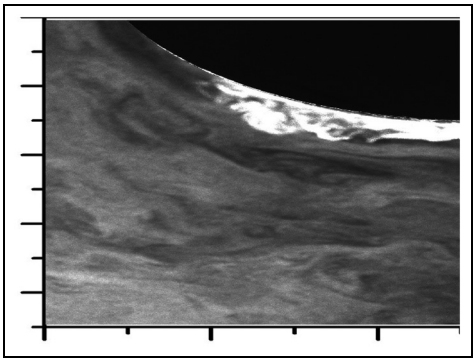

Figure 4. PIV measurements.

M = 0.75 increases and the velocity peaks present the same pattern from the jet exit for all span locations. The velocity variations decrease at M = 1, but on the other side, the frequency with which they occur increases as at C1where two peaks can be observed. This trend was observed also at M = 0.75 but only at C4. For blowing ratios M > 1, fluctuations decrease significantly and peaks raise around 25% of the mainstream velocity, except for C4 which increases with the blowing ratio.

Velocity contours along span positions are shown in Figures 6–10. Downstream the jet exit, mainstream accelerated drastically as blowing ratio decreased below M < 1. For the case of M = 0.5 (Figure 6), uniform velocities assure that cooling flow remains attached to the surface without separation of the film cooling layer. However, the layer thins at C4 due to an increase in blowing ratio which can be assumed like a reduction in pressure of the coolant flow causing a penetration of the mainstream into the film layer. The highest velocity is located downstream stagnation region at C4. At M = 0.75 (Figure 7), the flow remains attached to the surface blade in all span positions. A recirculation zone was observed near the stagnation region. A recirculation zone appears also at M = 0.5 with a pronounced velocity difference in the core of the vortex between span positions, whereas that difference diminishes at M = 0.75. Also, a reduction in the film layer thickness was observed at M = 0.75. Previous facts are due to a more uniform distribution of flow inside the plenum. The maximum velocity increases slightly, and peaks of velocity occur at C3 and C4.

The case of M = 1 confirms the development of the secondary CRVP around the film layer at C1 and C2.

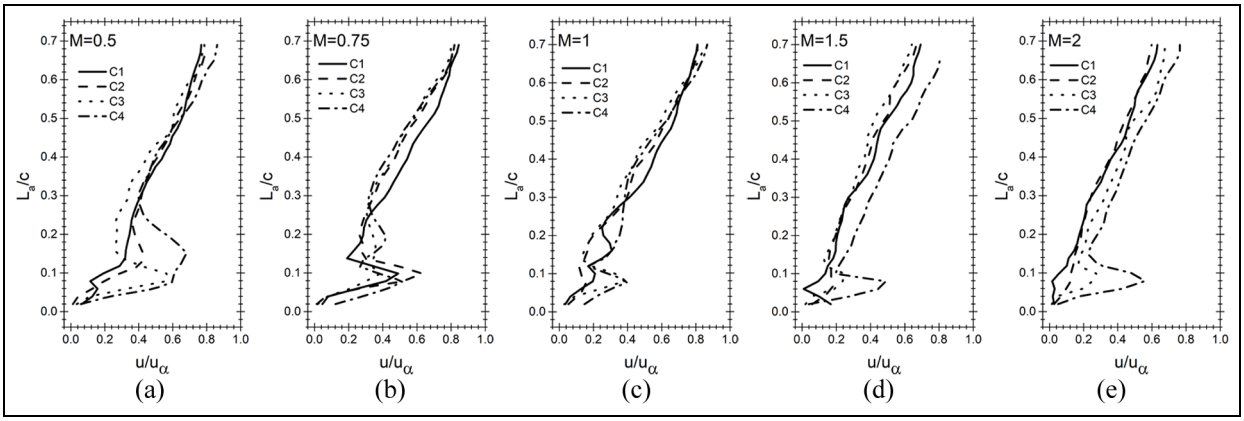

Figure 5. Velocity from the jet exit to the mainstream at different blowing ratios: (a) M = 0.5, (b) M = 0.75, (c) M = 1, (d) M = 1.5, and (e) M = 2.

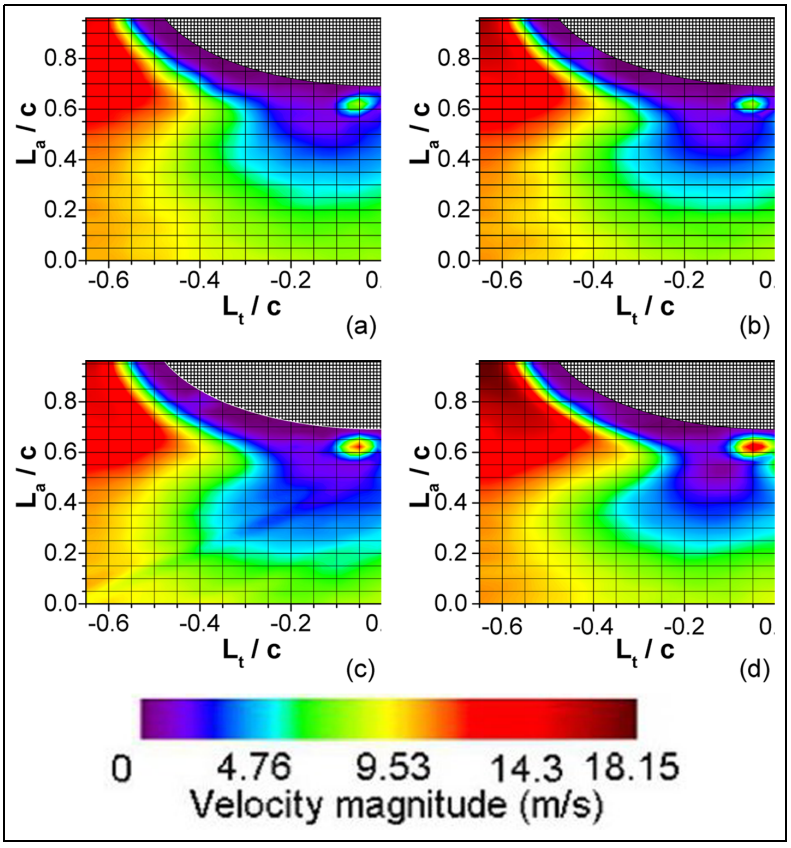

Figure 6. Velocity contours at M = 0.5: (a) C1, (b) C2, (c) C3, and (d) C4.

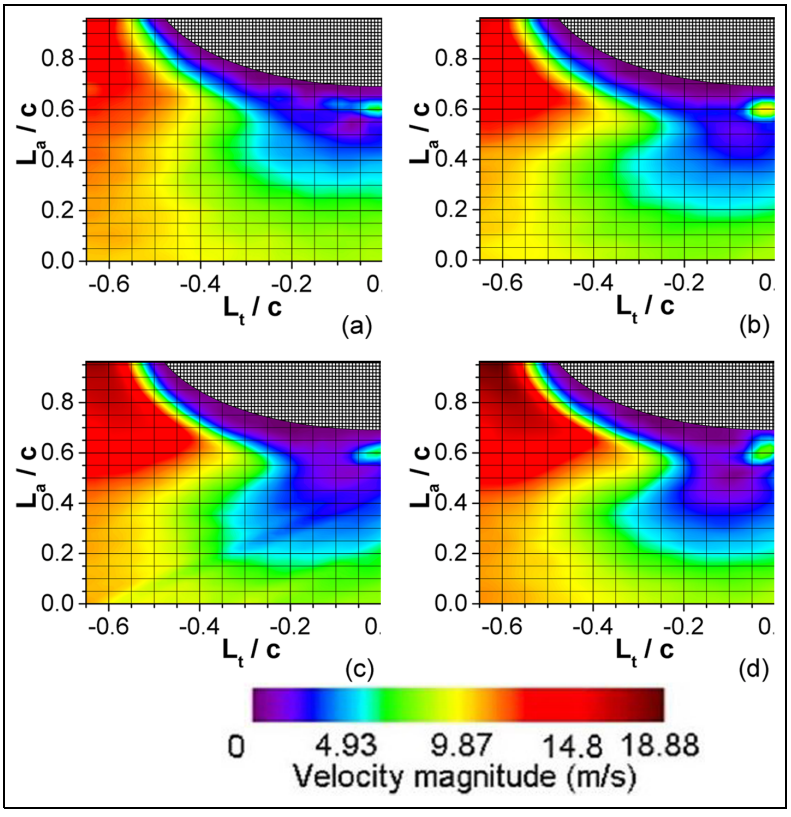

Figure 7. Velocity contours at M = 0.75: (a) C1, (b) C2, (c) C3, and (d) C4.

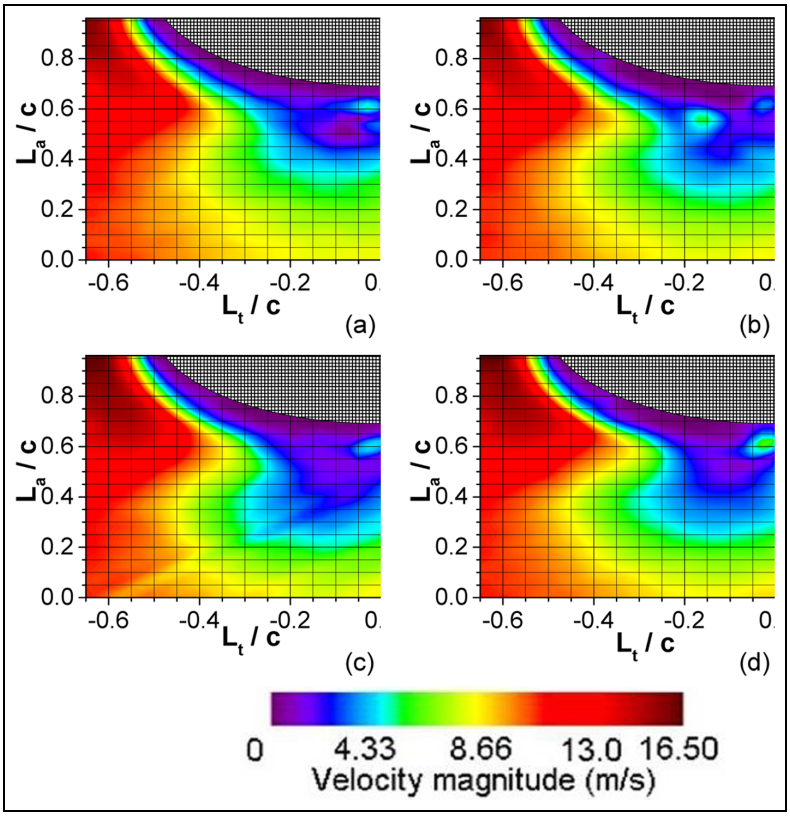

Figure 8. Velocity contours at M = 1: (a) C1, (b) C2, (c) C3, and (d) C4.

The peak velocity was reduced with respect to M = 0.5 and M = 0.75; nevertheless, at all locations, regions with maximum velocity were observed indicating a more uniform velocity distribution around the entire blade. Unlike M = 0.5 and M = 0.75, velocity in the core of vortex structure is significantly lower.

From the results of velocity at M = 1 (Figure 8), it is expected that increasing blowing ratio, remarkable perturbations will take place at the stagnation region near wall blade. This is verified in Figures 9 and 10 which represent velocity contours at M = 1.5 and M = 2. Regarding C1, at both blowing ratios, the flow is detached from the blade wall, whereas at C2, it is detached only at M = 2; nevertheless, the film layer is drastically reduced at M = 1.5. At C3 and C4, it remains attached to the surface. The detachment from the blade surface is predictable if blowing ratio increases. Small differences around 11.5 m/s in maximum velocity were found between M = 1.5 and M = 1.2.

The best conditions for a good film cooling performance can be found at M = 0.5 and M = 0.75 due to the attachment of film layer to the blade surface, whereas at M = 1, M = 1.5, and M = 2, a poor performance is expected due to the separation of cooling flow from the blade surface at stagnation region and its penetration into the mainstream. However, the peaks of velocity near the blade wall indicate that vortex structures can affect the cooling effectiveness. The contours show a decrease in the velocity intensity of the mainstream as consequence of an increase in the blow ratios; this is due to the interaction of the coolant jet, mainstream, turbulence, and vorticity.

Turbulence intensity profiles at 0.25D and 0.5D around leading edge and downstream of cooling discharge for all span positions are presented in Figure 11. In all cases, peaks of turbulence intensity are observed close to exit holes and as the flow moves away from exit holes, turbulence intensity diminishes. Slight increments occur at C2, C3, and C4 which can be caused by the influence of the jet of previous holes. However, these increments diminish but still occur at 0.5D. Higher turbulence intensity magnitudes appear at 0.5D being in some cases, at the same span, more than twice than 0.25D. On the basis, lower turbulence levels are expected in the zone where film cooling discharge occurs. The profile located at 0.25D showed that at C1 and C4 the maximum turbulence is developed when M = 0.5, whereas at C2 and C3 it is significantly reduced. It was observed that when M = 0.75, at C1 and C4, turbulence peaks occur just at exit hole, whereas at M = 1, this trend is repeated but at all span positions. When the blowing ratio is M = 1.5, higher turbulence appears at C1 and C4 and it diminishes

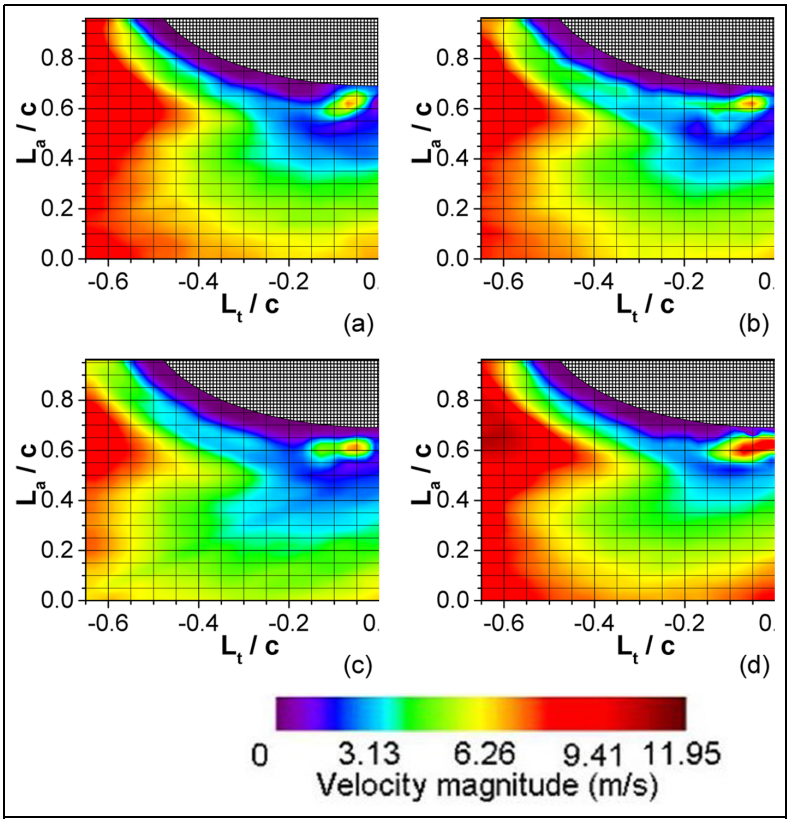

Figure 9. Velocity contours at M = 1.5: (a) C1, (b) C2, (c) C3, and (d) C4.

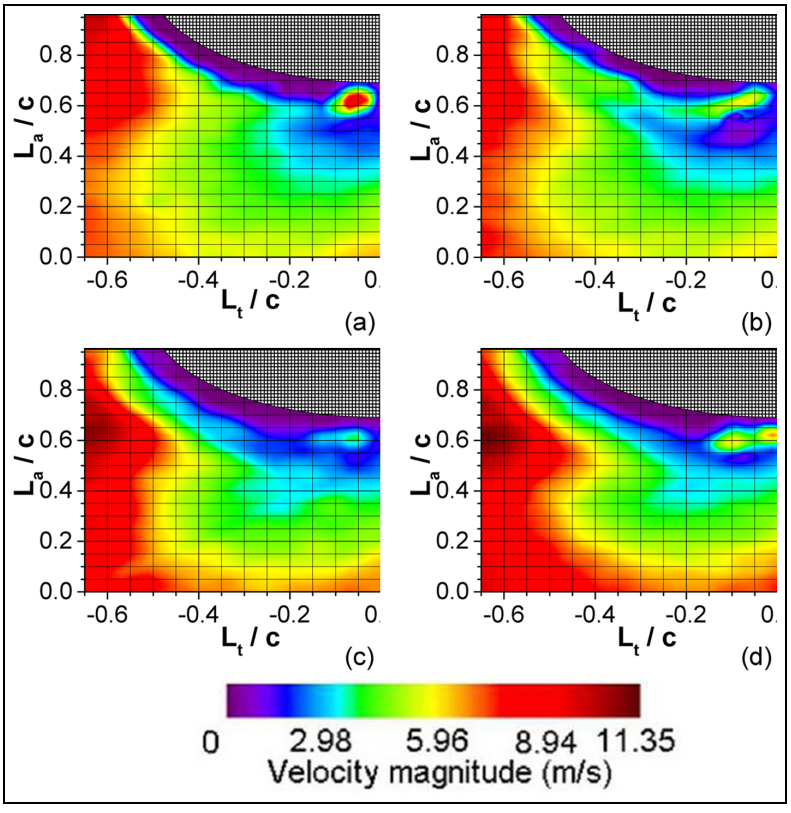

Figure 10. Velocity contours at M = 2: (a) C1, (b) C2, (c) C3, and (d) C4.

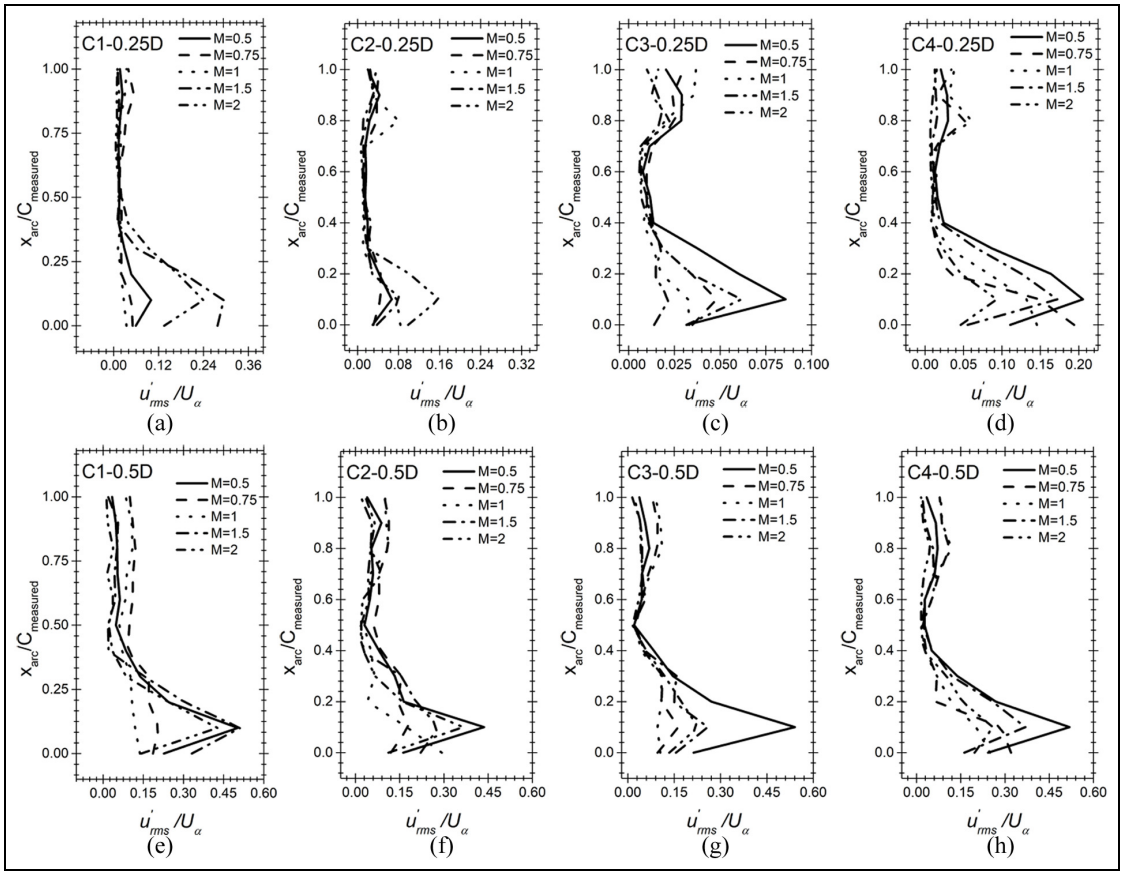

Figure 11. Turbulence intensity profiles: top row at 0.25D: (a) C1, (b) C2, (c) C3, (d) C4, and bottom row at 0.5D (e) C1, (f) C2, (g) C3, and (h) C4.

among them. Turbulence in both profiles with M = 2 was decreased as a function of the span.

In general, near the blade surface (0.25D), C4 presents high turbulence levels due to the influence of the pressure generated at the upper wall of the wind tunnel. Variations of turbulence along span were attributed to an even distribution of coolant flow at hole cavities as a function of blowing ratio. The higher the blowing ratios, the greater amount of coolant flow is ejected through the first holes of the row causing peaks of turbulence downstream of it, whereas at lower blowing ratios, it is supposed that the concentration of coolant flow occurs about halfway up.

Figures 12–16 present contours of vorticity for all proposed values of M at all span positions. Blue color indicates that vortices are rotating in the clockwise direction and red color indicates an anti-clockwise direction. In most cases, CRVP structures are observed at the stagnation zone. This is because the velocity gradients are higher at these zones and they lead to the formation of CRVP. The previous affirmation coincides with the results observed in the velocity contours. Downstream the jet exit, over the blade surface, there is no evidence of vortices that disturbed the film layer which indicates favorable pressure gradients in the near wall region. However, the radius around the blade, where vortex magnitudes are higher, decreases drastically from M = 0.75. Secondary vortices are observed at M = 1, M = 1.5, and M = 2 which reveals that coolant flow penetrates the mainstream and the increment of velocity gradients between both fluids. This has negative effects causing aerodynamic losses. At M = 0.5 and M = 0.75, at C1 and C2 span positions, the core of CRVP does not appear over blade surface at jet exit due to a favorable velocity gradient over it. This effect changes as blowing ratio increases. Minimal vortices appear at M = 0.5; however, their magnitude is greater than the other blowing ratios analyzed.

The obtained results have shown significant changes in the interaction of mainstream with cooling flow through span length. These changes are mainly due to mainstream flow conditions and have an impact on film cooling. If the study is performed on flat plates, the behavior of the interaction through span cannot be observed due to the nature of the experimental array. In addition, the leading edge curvature, which also influences the flow field, is well represented in the cylindrical model, which is the importance of this research.

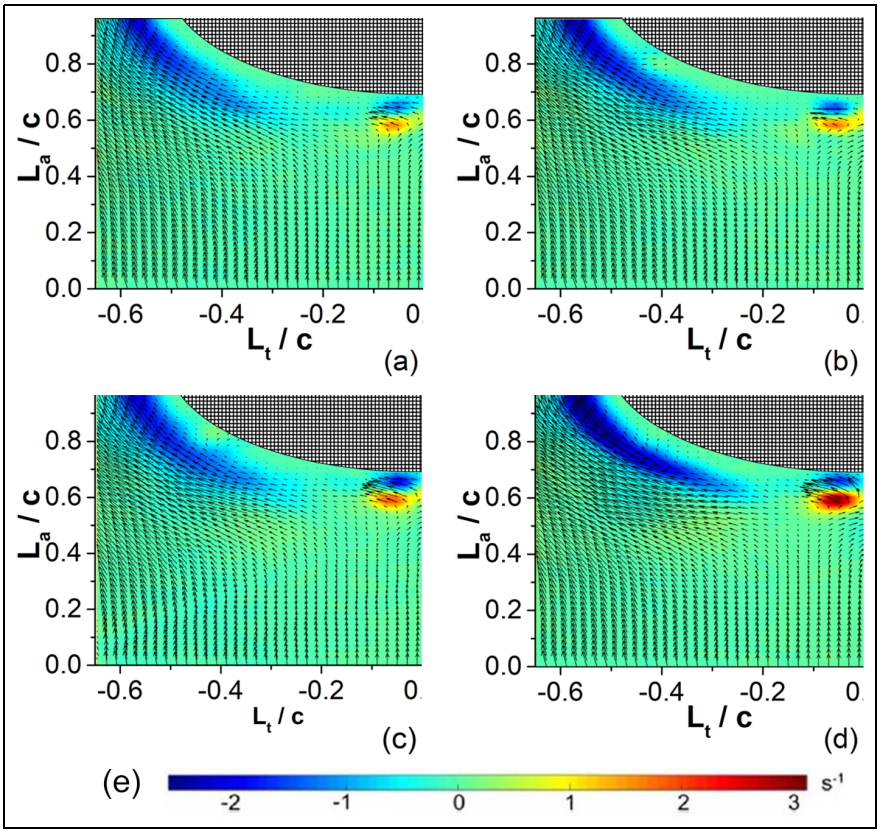

Figure 12. Vorticity contours at M = 0.5: (a) C1, (b) C2, (c) C3, (d) C4, and (e) scale.

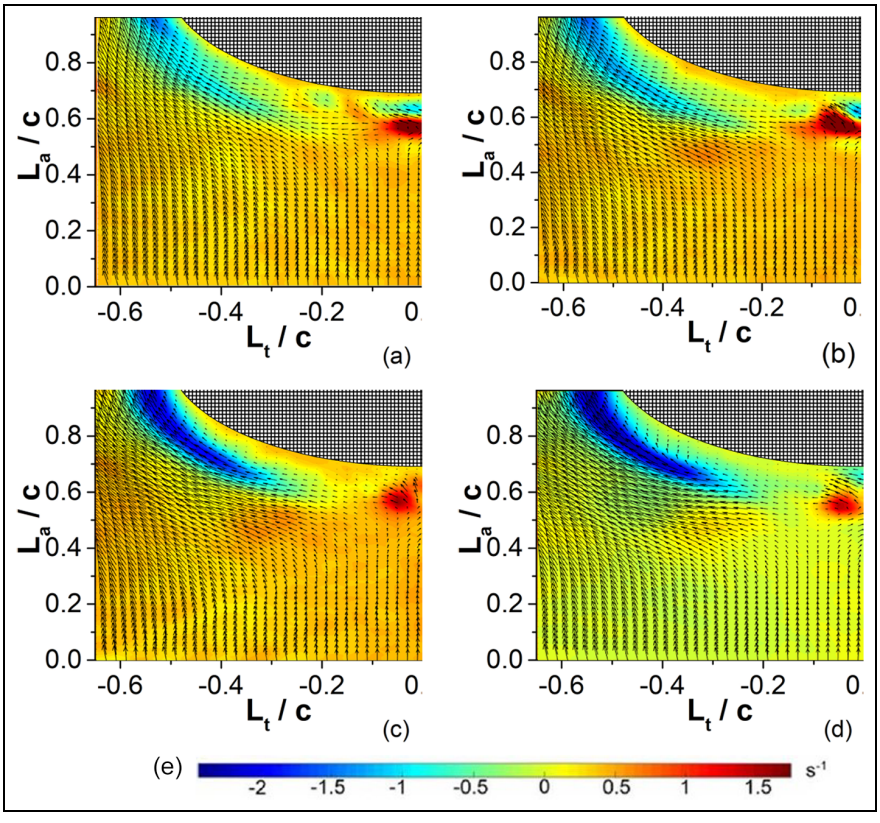

Figure 13. Vorticity contours at M = 0.75: (a) C1, (b) C2, (c) C3, (d) C4, and (e) scale.

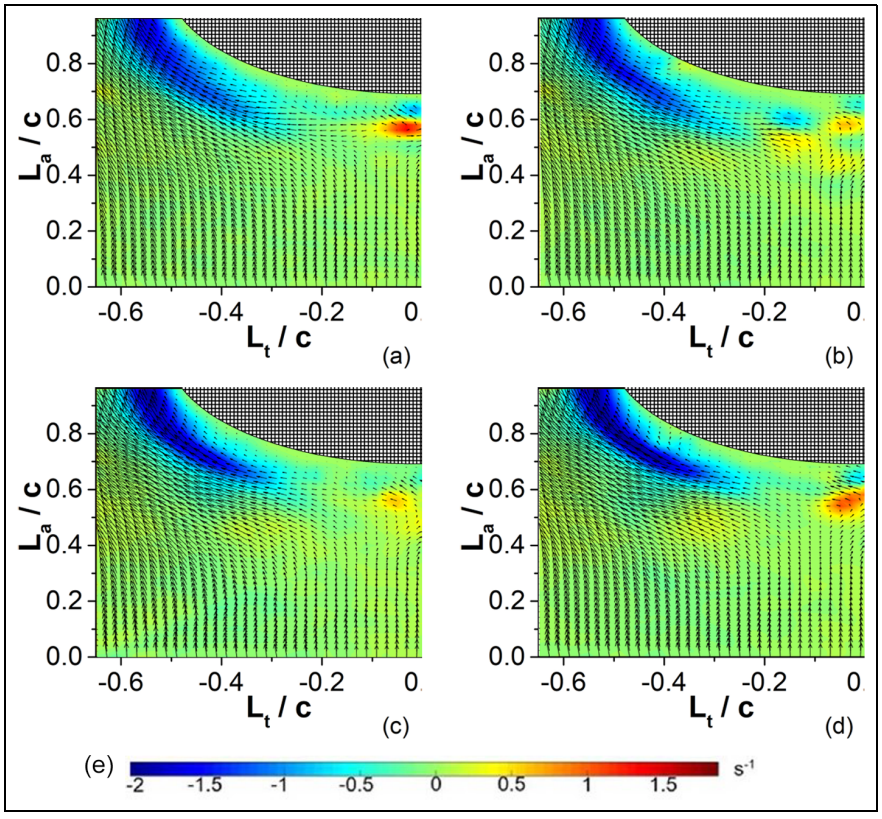

Figure 14. Vorticity contours at M = 1: (a) C1, (b) C2, (c) C3, (d) C4, and (e) scale.

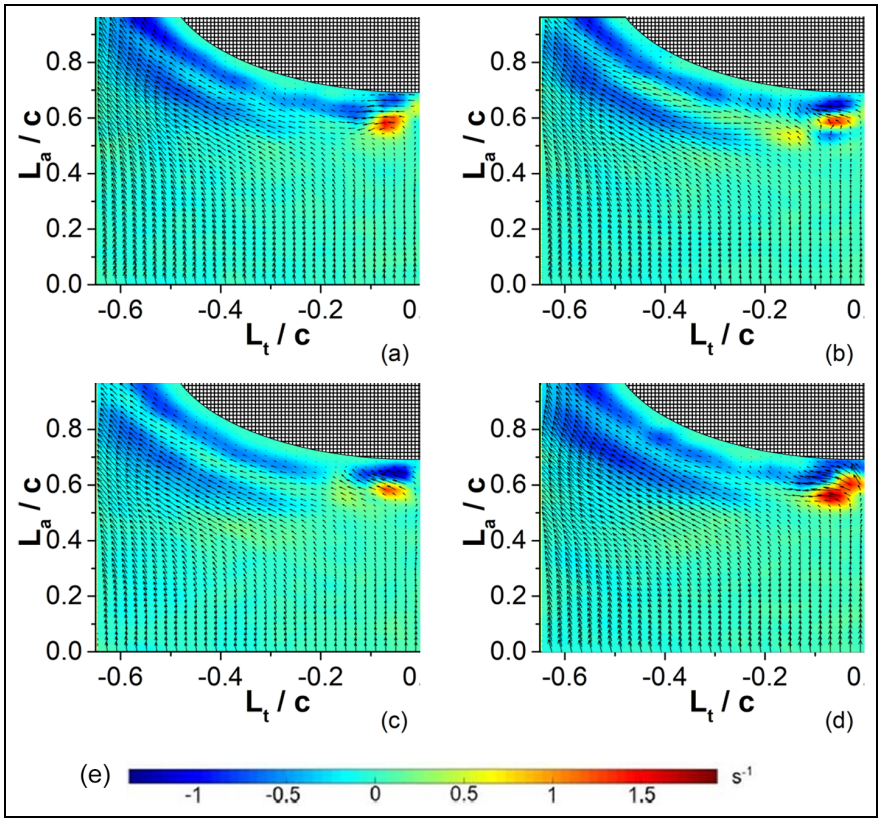

Figure 15. Vorticity contours at M = 1.5: (a) C1, (b) C2, (c) C3, (d) C4, and (e) scale.

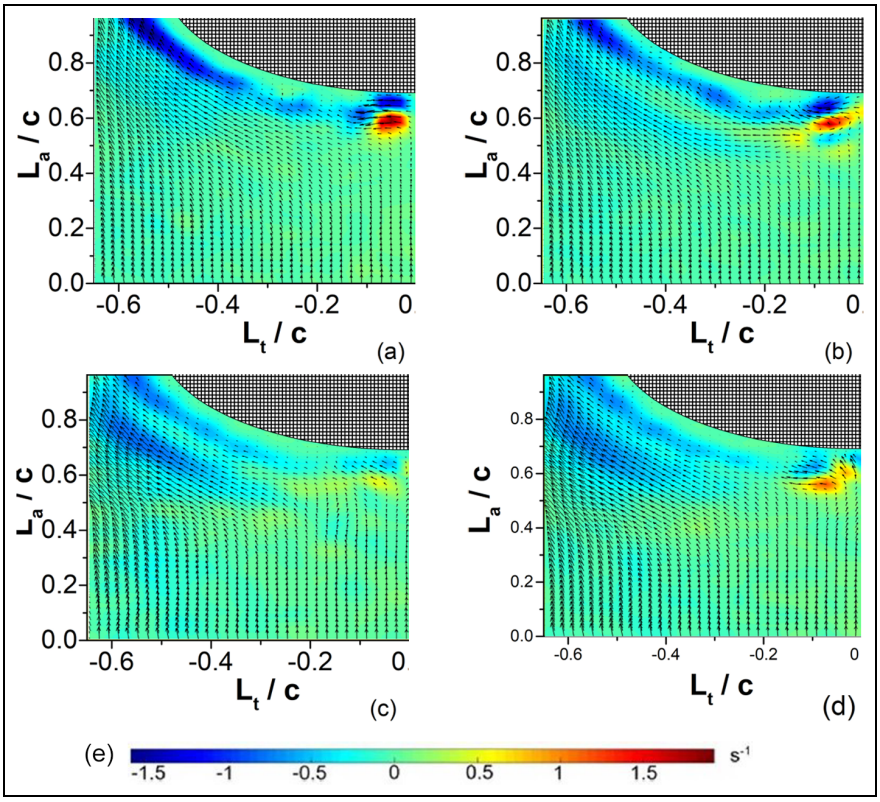

Figure 16. Vorticity contours at M = 2: (a) C1, (b) C2, (c) C3, (d) C4, and (e) scale.

Conclusion

In this study, PIV measurements were carried out to study the flow field around a film-cooled turbine blade leading edge along the span at different blowing ratios. The results showed that downstream the jet exit, mainstream accelerates drastically as blowing ratio decreases, $M < 1$, and span increases. For the blowing ratios $M = 0.5$ and $M = 0.75$, the flow remains attached to the blade surface, while at higher blowing ratios, $M > 0.75$, the cooling flow breaks the cooling layer causing penetration into the mainstream and generation of velocity gradients. Turbulence intensity was measured in two positions around gas turbine blade leading edge at 0.25D and 0.5D.

Around the periphery of the blade leading edge, high turbulence levels were found. The turbulence peak was found in the zone located between the mainstream and the film cooling, except for blowing ratio $M = 1$; in this case, the peak occurs exactly at the cooling flow discharge.

Turbulence is large at low- and high-span values due to the effects of pressure between the lower and upper walls of the flow channel. The coolant flow distribution is affected by the blowing ratios and also it influenced the magnitudes of turbulence. Downstream the jet exit, turbulence increments were caused by the remaining jet from previous cooling holes. The presence of CRVP at the stagnation zone was documented. For $M = 0.5$, CRVP was minimal but its magnitude was greater than at other blowing ratios. Secondary vortices appeared due to velocity gradients at higher blowing ratios, $M > 1$, and caused aerodynamical losses.

Declaration of conflicting interests

The author(s) declared no potential conflicts of interest with respect to the research, authorship, and/or publication of this article.

Funding

The author(s) received no financial support for the research, authorship, and/or publication of this article.

ORCID iD

José Omar Dávalos Ramírez https://orcid.org/0000-0002-6612-5231

References

1. Liu C, Zhu H, Zhang X, et al. Experimental investigation on the leading edge film cooling of cylindrical and laid-back holes with different radial angles. *Int J Heat Mass Tran* 2014; 71: 615–625.

2. Baldauf S, Schulz A and Wittig S. High-resolution measurements of local heat transfer coefficients from discrete hole film cooling. *J Turbomach* 2001; 123: 749–757.
3. Bidan G, Vézier C and Nikitopoulos DE. Study of unforced and modulated film-cooling jets using proper orthogonal decomposition: part I: unforced jets. *J Turbomach* 2012; 135: 021037.
4. Renze P, Schröder W and Meinke M. Large-eddy simulation of film cooling flows at density gradients. *Int J Heat Fluid Fl* 2008; 29: 18–34.
5. Rozati A and Tafti DK. Large-eddy simulations of leading edge film cooling: analysis of flow structures, effectiveness, and heat transfer coefficient. *Int J Heat Fluid Fl* 2008; 29: 1–17.
6. Liang JY and Kang S. Investigation of film cooling on the leading edge of turbine blade based on detached eddy simulation. *Sci China Technol Sc* 2012; 55: 2191–2198.
7. Zhang S, Qin J, Bao W, et al. Numerical analysis of supersonic film cooling in supersonic flow in hypersonic inlet with isolator. *Adv Mech Eng* 2014; 6: 1–9.
8. Walters DK and Leylek JH. A detailed analysis of film-cooling physics: part I: streamwise injection with cylindrical holes. *J Turbomach* 1997; 122: 102–112.
9. Shi HH, Kiriyama K and Itoh M. Hot wire measurement of turbulent boundary layer on a film cooling plate with diffusion holes. *J Hydrodyn* 2001; 13: 15–23.
10. Pomfret JR, Guo SM, Oldfield MLG, et al. A high-speed concentration probe for the study of gas turbine vane film cooling. *Meas Sci Technol* 2002; 13: 1966–1973.
11. Womack KM, Volino RJ and Schultz MP. Measurements in film cooling flows with periodic waves. *J Turbomach* 2008; 130: 041008.
12. Pietrzyk JR, Bogard DG and Crawford ME. Hydrodynamic measurements of jets in crossflow for gas turbines film cooling applications. *J Turbomach* 1989; 111: 139–145.
13. Pietrzyk JR, Bogard DG and Crawford ME. Effects of density ratio on the hydrodynamics of film cooling. *J Turbomach* 1990; 112: 437–443.
14. Thole K, Gritsch M, Schulz A, et al. Flowfield measurements for film-cooling holes with expanded exits. *J Turbomach* 1998; 120: 327–336.
15. Eberly MK and Thole KA. Time-resolved film-cooling flows at high and low density ratios. *J Turbomach* 2013; 136: 061003.
16. Wright LM, McClain ST and Clemenson MD. Effect of freestream turbulence intensity on film cooling jet structure and surface effectiveness using PIV and PSP. *J Turbomach* 2011; 133: 041023.
17. Zheng Y and Hassan I. Experimental flow field investigations of a film cooling hole featuring an orifice. *Appl Therm Eng* 2014; 62: 766–776.
18. Song L, Zhang C, Song Y, et al. Experimental investigations on the effects of inclination angle and blowing ratio on the flat-plate film cooling enhancement using the vortex generator downstream. *Appl Therm Eng* 2017; 119: 573–584.
19. Zhou W and Hu H. Improvements of film cooling effectiveness by using Barchan dune shaped ramps. *Int J Heat Mass Tran* 2016; 103: 443–456.
20. Kukutla PR and Prasad BVSSS. Secondary flow visualization on stagnation row of a combined impingement and film cooled high-pressure gas turbine nozzle guide vane using PIV technique. *J Visual Japan* 2017; 20: 817–832.
21. Forliti DJ, Strykowsky PJ and Debatin K. Bias and precision errors of digital particle image velocimetry. *Exp Fluids* 2000; 28: 436–447.